Journal of Engineering and Applied Sciences 12 (6): 1641-1648, 2017
ISSN: 1816-949X

Numerical Analysis of the Laminar Pulse Flow within Fractures with Penetrable Walls

Nader Pourmahmoud and Aidin Zabihi
Department of Mechanical Engineering, Urmia University, Urmia, Iran

Abstract: In many geological structures, the permeability or penetrability of stone matrix is negligible compared to stone fracture. In fact, fractures are the main direction of flow in stone massifs. As a result of improving the efficiency of design studies; implementation of barefaced underground structures; separation of carbon dioxide in underground brines; disposal of nuclear waste and investigation of the behavior of the current within the fracture is considered as a crucial research project. The present study elaborates on a calculative model for single-phase flow in a fractured environment in a special situation. The geometry of the fracture under study is obtained through a series of Ct-scans from real fractures in Berea sandstone. The Ansys-Fluent Software analyses the flow within a fracture with flow rate of 0.312-31.2 mm^2/sec and width and permeability unit of 500 mm Darcy and through application of pulse-sine input rate. Flow condition and pressure drop calculated in this study are compared with a simulation of walls of an impenetrable fracture. The calculated fracture range is produced through a two dimensional stone matrix. Furthermore, laminar flow is calculated for several input rates. The pressure drop within the fracture is used to describe the relationship between flow rate and pressure drop resulting from flow.

Key words: Porous environment, single-phase flow, laminar flow, friction coefficient, Reynolds number

INTRODUCTION

Several significant advances have taken place in the context of mathematical modeling of flow within fractures since 1960's. In addition, several research efforts have been made in order to improve the development and efficiency of oil reservoirs and other natural resources and in order to eliminate the concerns for undersurface pollutions. In fact these efforts have provided the necessary contexts for development of several numerical and technical modeling methods Lomize (Barenblatt *et al*., 1960). The cubic law of laminar flow within a canal surrounded by two parallel glass sheets has been empirically validated. However, in real geological conditions it is extremely hard to find a fracture with flat surface, i.e., most natural stone fractures are uneven and adopt variable spatial diaphragms. The linear form of the Darcy rule has been extensively used for description of laminar flows at low rates (Court-Brown and McQueen, 2002). Researchers have investigated several conceptual models for comparison of the model of fracture matrix interaction, in fractured porous environments (Berkowitz, 2002). Investigation of movement of water and other fluids within unsaturated earth materials has resulted in several accomplishments including disposal of dangerous wastes in deep areas of earth, increased oil recovery, extraction of shale gas and other structures, advances in nuclear magnetic resonances and advanced applications of x-ray in imagery technologies, etc. Our empirical knowledge regarding imagination of fracture flow within saturated porous environments is a crucial item. Currently researchers are able to determine water movement and distribution in a wide range of natural and engineering materials in different spatial and temporal resolutions. In many geological structures the permeability or penetrability of stone matrix is negligible compared to stone fracture. In this situation the hydraulic behavior of the stone massif is controlled by fractures. Therefore, comparison and estimation of the hydraulic behavior of stone massif requires a suitable understanding of the hydraulic behavior of the fracture and fracture networks. By making use of a suitable hydraulic model for investigation of hydraulic behavior of stone massifs, design and safety studie's precision can be improved for surrounding environments of underground pores such as tunnels and nuclear waste repositories. In terms of microscopic scales, the behavior of fluid flows within fractures is expressed by the use of Navier-Stokes non linear partial derivatives (Zimmerman and Bodvarsson, 1996). In general, these equations are extremely difficult to solve and simultaneously, complexity of the geometry of fracture adds up to this difficulty. Primary studies for generalization of the Darcy's (cube) law for real fractures were performed using empirical data (Louis, 1969). Navier Stokes equationsare capable of providing a well-defined description of movement of flow

Corresponding Auithor: Nader Pourmahmoud, Department of Mechanical Engineering, Urmia University, Urmia, Iran

Fig. 1: Dimensional schematic of the fracture

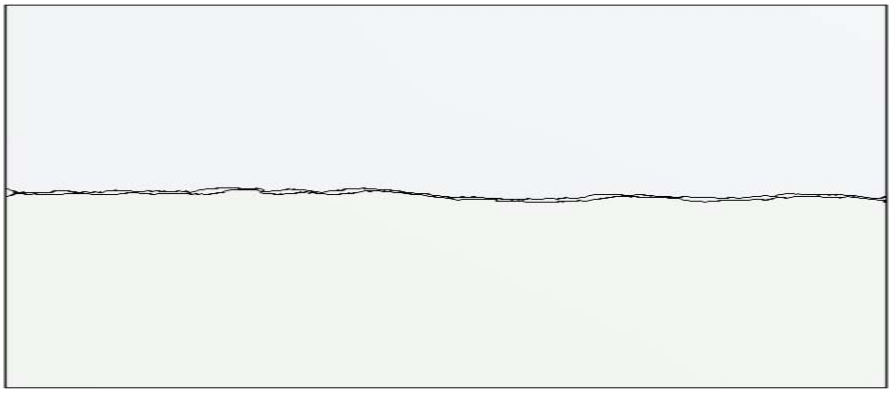

Fig. 2: The schematic of the fracture along with its surrounding matrix

in different scales. In fact non-linear equations may result in extension of calculation time. Suitable pre conditions for making desirable engineering predictions have stimulated macroscopic empirical development. Darcy's law is extensively used for investigation of behavior of flow within fractures. With respect to the geometric shape of the sample of interest, different researchers have made use of various geometric profiles with uneven parallel w alls including saw tooth (Elsworth and Goodman, 1986) sinusoidal and stepped (Tsang and Witherspoon, 1981; Neuzil and Tracy, 1981). In aforementioned conditions, the hydraulic behavior of the fracture is inspected using effective opening. Flow systems and non-linear flows in fractures have been empirically (Louis, 1969) experimentally (Qian *et al*., 2005) and numerically (Koyama *et al*., 2008) investigated by different researchers. Since, Reynold's equation's efficiency is considerably insufficient in these cases more recently the numerical calculation of the Navier-Stokes equation is used for investigation of fluid flows within fractures (Brush and Thomson, 2003; Koyama *et al*., 2008). In many studies, the non-linear behavior of flow within fractures has been expressed by the use of Brinkman-Forchheimer equation (Elsworth and Goodman, 1986; Zimmerman *et al*., 2004; Chenz *et al*., 2001). The aforementioned equation expresses the relation between pressure drop and the flow rate through the fracture in terms of a quadratic polynomial.

Entire previously mentioned research efforts have improved our knowledge in terms of non-linear behavior of flows. The present article has elaborated on numerical calculation of the Navier-Stokes equation for a viscose fluid in a laminar and two-dimensional flow within a fracture with the use of ansys fluent: CFD simulation software. In addition, the flow in the fabricated fracture has been simulated by. Furthermore, in order to achieve a constant flow rate at the opening of fracture, pressure drop has also been calculated along with penetrability matrix. In order to investigate the effect of penetrability of matrix of surroundings of fracture on the flow, the aforementioned matrix was investigated thoroughly. Nevertheless, an equation has also been yielded for friction coefficient of the fracture. A porous matrix with porosity of 20% has been considered for non-deformable walls (Fig. 1 and 2).

The equations governing the flow: Overall description of fluid flow within a fracture is done through application of Navier-Stokes relations. These relations or so-called equations express the momentum and mass balance in fracture space. Considering a stable and laminar flow and a Newtonian fluid with constant viscosity and density within a fracture with impenetrable walls, the Navier-Stokes equations can be re-written in the following vector form (Zimmerman *et al*., 2004):

$$\rho)u.\nabla(u = \mu - \nabla^2 u \nabla p \quad (1)$$

In the upper equation, "ρ" represents the density of fluid; represents the viscosity of the fluid; "μ" represents the rate flow vector and "ρ" represents the Hydrodynamic pressure.

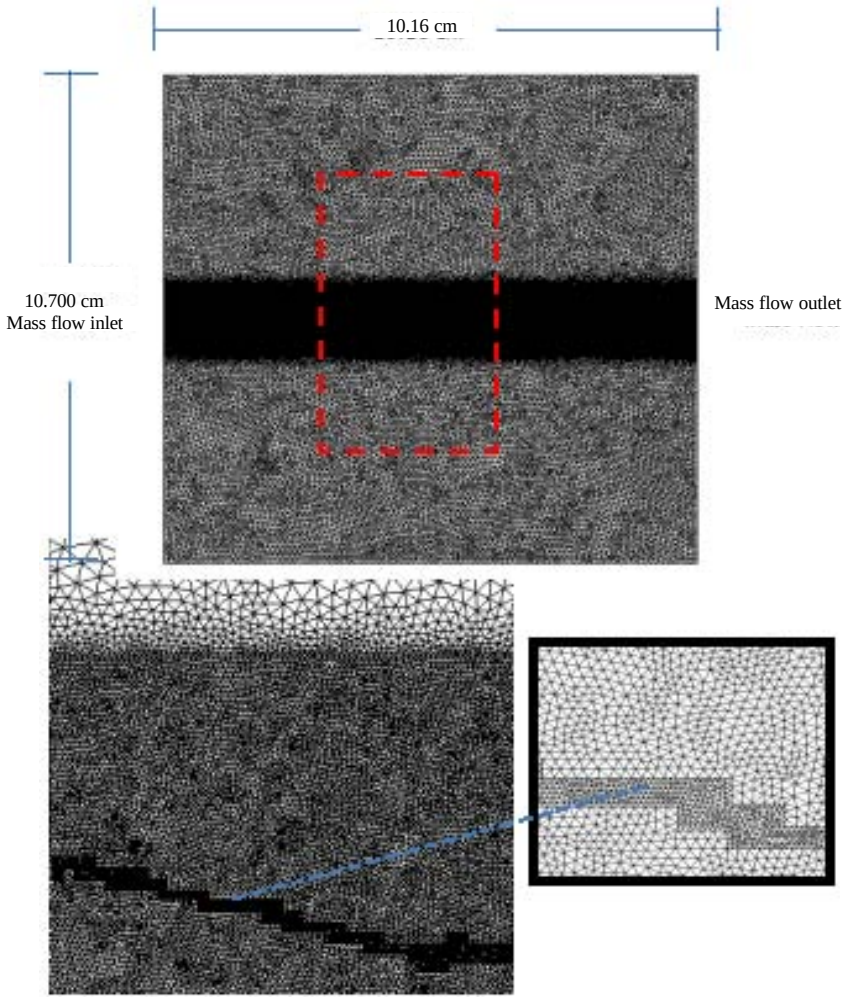

Fig. 3: Schematic of fracture shape geometry

In order to have a package of equations (Chen *et al*., 2001) we are required to combine these equations with continuity equations (which express the mass balance) (Zimmerman and Bodvarsson, 1996). For an incompressible fluid, the mass balance equation is equal to the volume balance equation. Therefore, it is re-written in the following form Nazridoust *et al*. (2006) (Fig. 3):

$$\nabla.u = 0 \quad (2)$$

MATERIALS AND METHODS

Model geometry: The fracture geometry used in this study is achieved through conversion of 3D data into 2D data through CT-Scan. This method was introduced by Nazirdoost *et al*. (2006) and was used in the long core of Berea sandstone. The preferred fracture is generated through distribution of tension in ways almost similar to standard Brazilian method (Chen *et al*., 2001). For a single-phase laminar flow, water fluid with density of 998.2 kg/m^3 and viscosity of 0.001 kg/msec and air with density of 1.225 kg/m^3 and viscosity of 1.8×10^{-5} have been assumed. For fracture with penetrable wall matrix; flow rate ranged between 0.312 mm^2/sec and 31.2 mm^2/sec per width unit. In addition sinusoidal pulse rate was applied with frequency of 1 time/sec and penetrability was assumed as 500 mm Darcy. It should be noted that rate was also applied with no pulse and no penetrability. In sum, a total of 16 simulations were run for water and air.

Boundary conditions: The marginal condition of input rate is used for the input area. The input rate is considered as monotonous and in line with X vector. In addition the marginal condition of the output flow is considered for the output of flow in the geometry of fracture. The other solid surfaces of the fracture (fracture boundaries) have been expressed as impenetrable walls with no-flow boundary conditions.

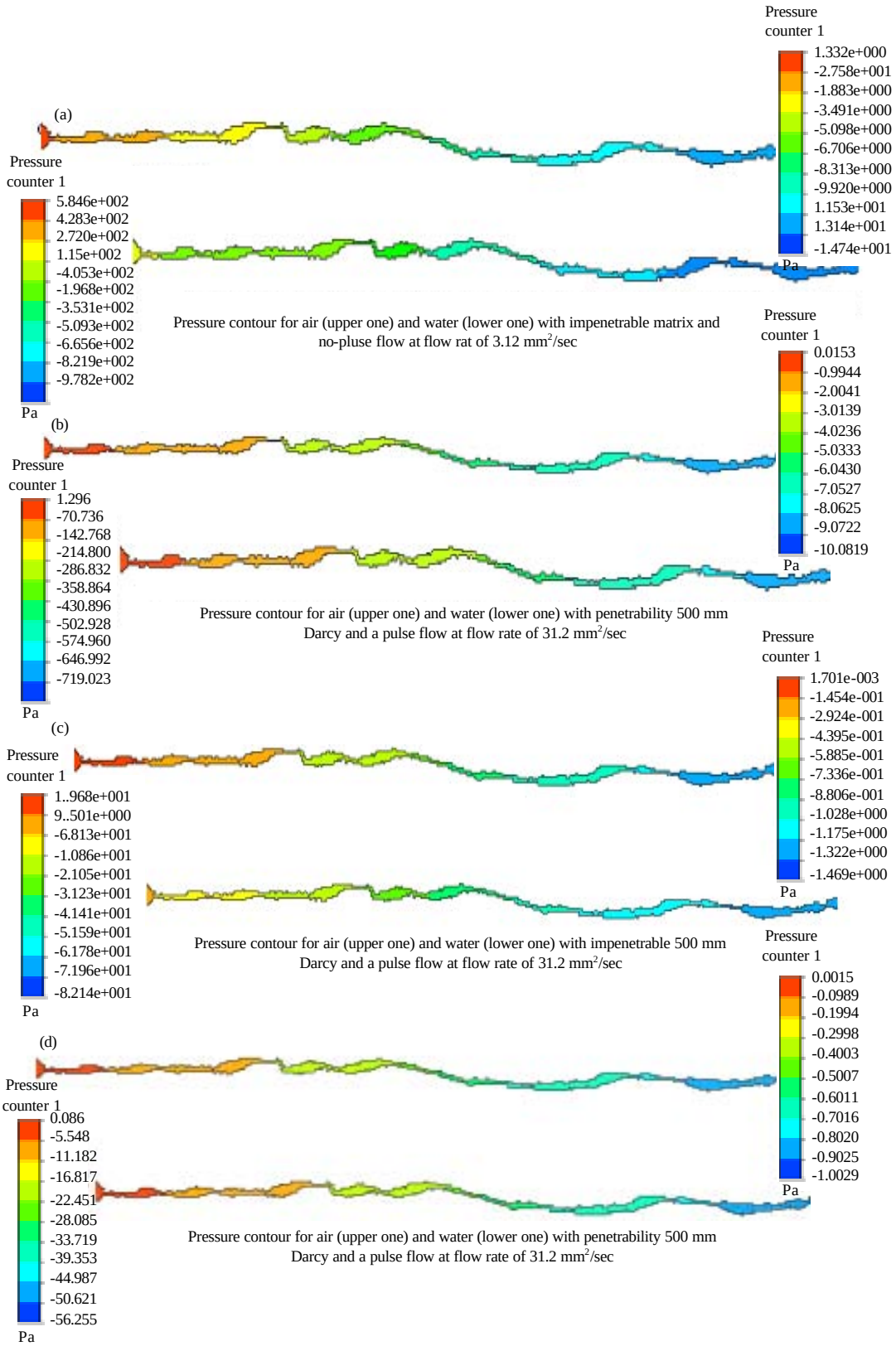

Fig. 4: Continue

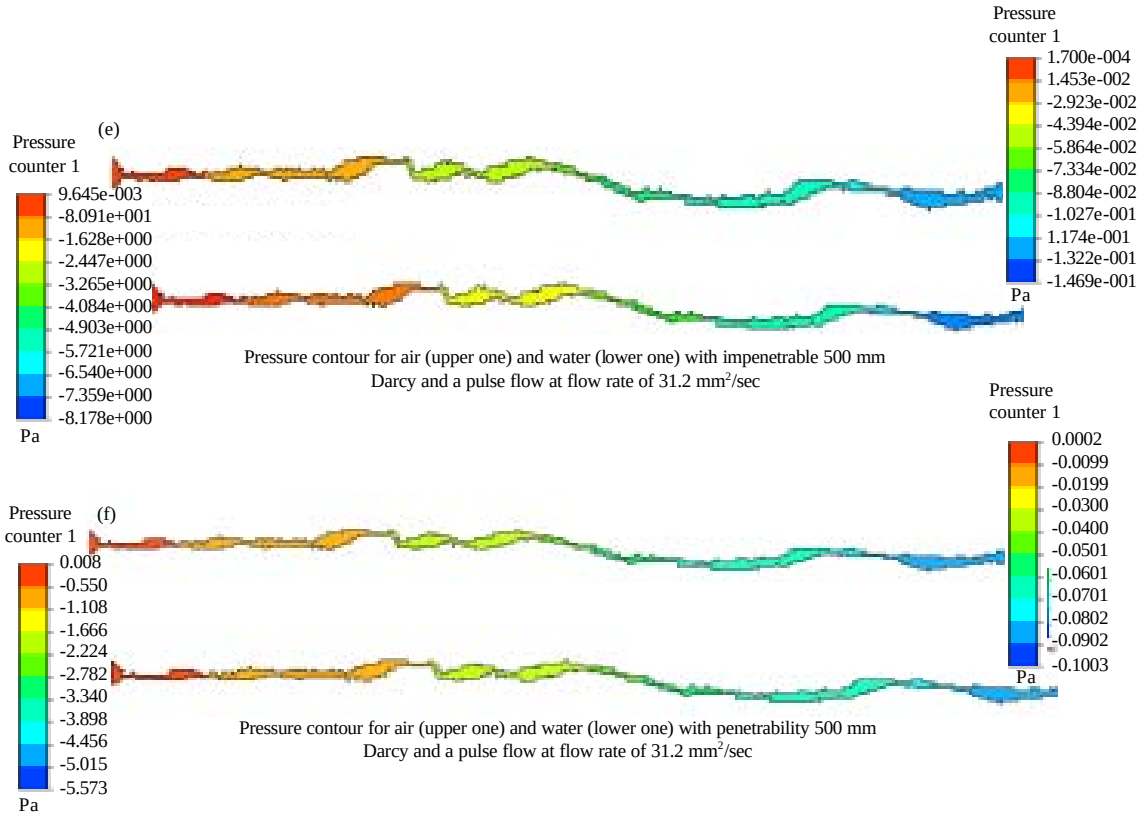

Fig. 4: Schematics of pressure contours for air and water flows under penetrability, impenetrability, pulse-flows and no-pulse flows

RESULTS AND DISCUSSION

Results of simulation: Single-phase flows of water and air were analyzed through fracture passages and the pressure-drop related to each different flow rate was investigated. The flow is considered as a laminar and incompressible one. Figure 4 shows the static pressure changes in fracture for the flow rate of water and air in the range between 0.312-31.2 mm^2/sec. This Fig. 4 shows a roughly linear change in pressure along the fracture. The pattern of pressure lines in this figure is similar to the flow of air in the fracture except that water pressure drop is much more than air's pressure drop. This is mostly due to water's higher viscosity compared to air (Viscosity ratio between water and air is 0.67). As you can see, similar to the case with air contour meters, the rate of pressure drop is directly related to the flow rate for water contour meters too. Considering for the matrix of surroundings of fracture has resulted in reduction of amount of fracture coefficient and pressure-drop. Logarithm diagrams show the logarithm of the relation between flow rate and pressure-drop.

Vector of rate for the flow rate of 3.12 mm^2/sec per fracture width unit is shown for both water and air flows. As you can see, the fluid is directed towards the high rate flow. The air's maximum flow rate is 228.5 mm/sec while for water the maximum rate can be 228.3 mm/sec (Fig. 5-8).

Air pressure drop for the flow rate of fracture at width unit of 0.312-31.2 mm^2/sec is between 0.1-20 Pa. The amount of dependence of more twist is present, highest pressure drops are expected. A considerable portion of pressure drop takes pressure drop on fracture opening is referred to as the cube law. As the opening of the effective fracture is smaller and place in areas with the smallest diaphragms. The following two vectors show the relationship between flow rate and pressure drop for fractures with penetrable and impenetrable matrixes and flows of water and air. As you can see as the flow rate increases, pressure drop increases in a linear form as well (Fig. 9 and 10). In a similar form, pressure-drop changes in fractured part are analyzed for water flow and results are shown in the following image. Pressure changes are between 8-1050 Pa in the range of flow rate of 0.312-31.2 mm^2/sec. It should be pointed out that in this range, the Reynold's number is variable too. Despite higher pressure drop in terms of the water flow the trend of changes in the flows are similar for water and air. As

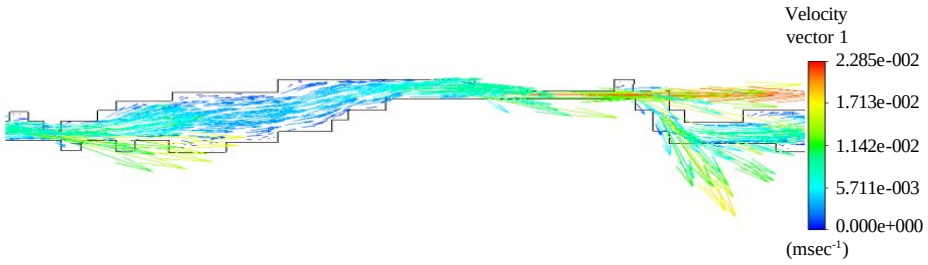

Fig. 5: Rate vector for air with impenetrable matrix and no-pulse flow at flow rate of 3.12 mm^2/sec

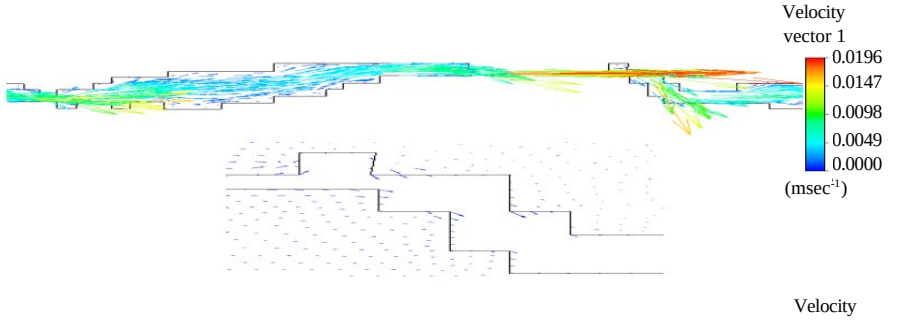

Fig. 6: Rate vector for air with penetrability of 500 mm Darcy and pulse flow at flow rate of 3.12 mm^2/sec

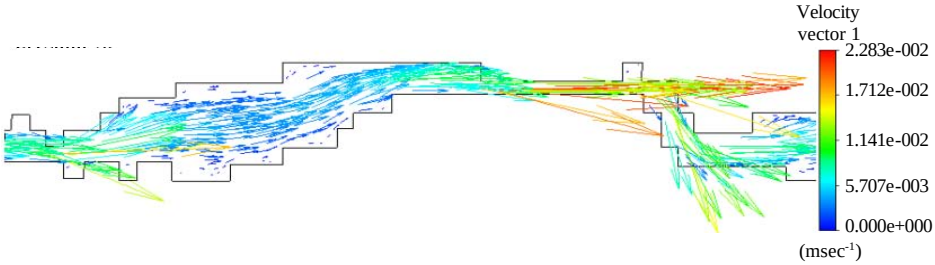

Fig. 7: Rate vector for water with impenetrable matrix and no-pulse flow at flow rate of 3.12 mm^2/sec

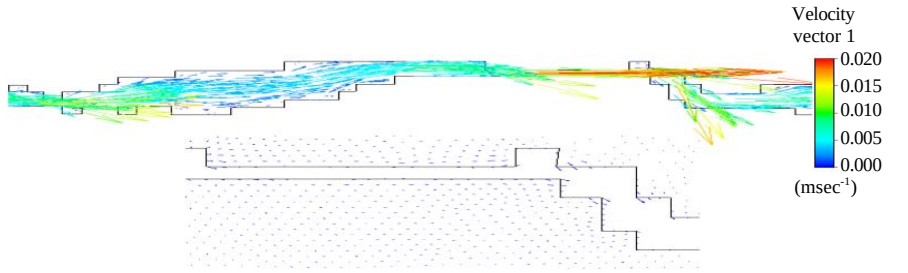

Fig. 8: Rate vector for water with penetrability of 500 mm Darcy and pulse flow at flow rate of 3.12 mm^2/sec

you can see in the diagram, the slope of the porous environment is almost equal to the slope of impenetrable wall. The calculated pressure drop for the porous environment and pulse flow is almost 31% less than pressure drop observed for impenetrable matrixes. Friction coefficient for a laminar flow between two parallel surfaces is as follows:

$$f = \frac{96}{Re_{\bar{H}}} \quad (3)$$

In terms of the upper equation, whenever the Reynolds number increases, the friction coefficient decreases. The Reynolds number is defined as follows:

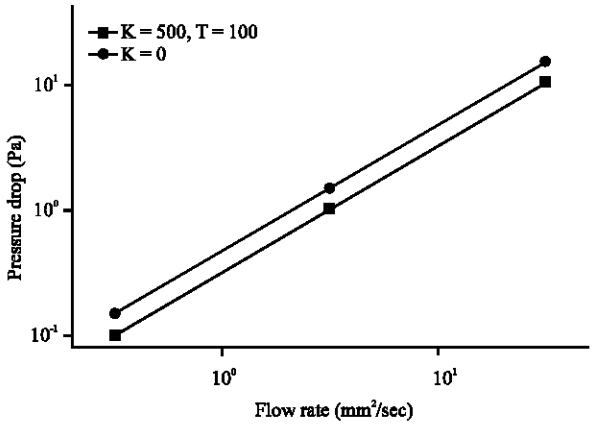

Fig. 9: Comparison of pressure drop per flow rate for air flow

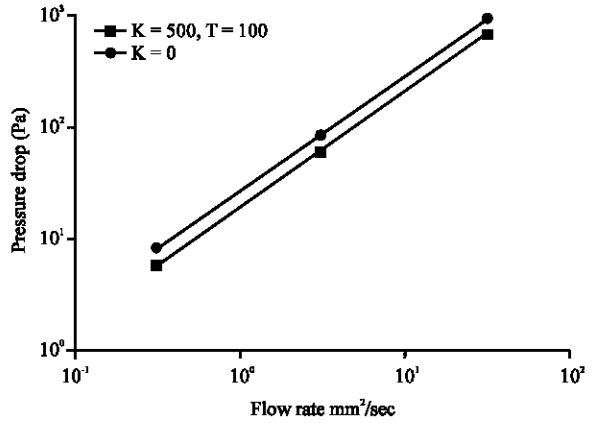

Fig. 10: Comparison of pressure drop per flow rate for water flow

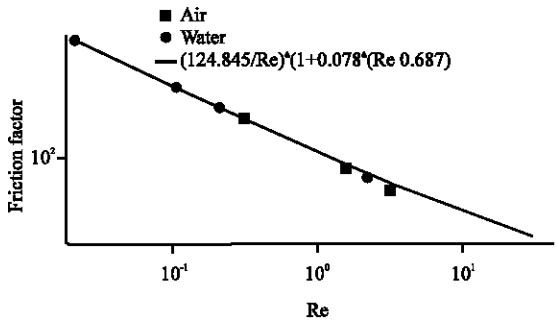

Fig. 11: Comparison of friction coefficients according to Reynolds number

$$Re_{\bar{H}} = \frac{\rho V_{\bar{H}}}{\mu} = \frac{\rho Q_f}{\mu} \quad (4)$$

Ultimately, a friction coefficient equation is obtained for this special fracture with impenetrable walls (Fig. 11):

$$f = \frac{124.845}{Re_{\bar{H}}}\left(1 + 0.078 Re_{\bar{H}}^{0.687}\right) \text{when } Re_{\bar{H}} \le 2 \quad (5)$$

Considering for porous environment surrounding the fracture along with a pulse flow-rate, results in a 31% pressure-drop. By making use of the results of simulations, a relationship has been developed for investigation of friction coefficient of a fracture surrounded by a penetrable matrix. On this basis, another new fracture friction coefficient is presented for fractures with penetrable porous matrixes:

$$f = \frac{83.456}{Re_{\bar{H}}}\left(1 + 0.078 Re_{\bar{H}}^{0.687}\right) \text{when } Re_{\bar{H}} \le 2 \quad (6)$$

Empirical equations number 5 and 6 provide a precise logical estimation of pressure-drop and friction coefficient for fractures and a wide range of Reynolds numbers that are smaller than 2. In terms of equations number 5 and 6, friction coefficient maintains its reverse relation with small Reynolds numbers. In fact the common non-linear dependence in Reynolds is because of laminar inertia effects in higher Reynolds numbers. Results of simulations under different conditions are in consistence with parallel surfaces model. The new empirical model for fracture friction shows that when the statistical knowledge regarding length of fracture and diaphragm are available, then pressure-drop becomes valuable as a function of flow rate in fractured reservoirs.

By making use of the Navier-Stokes equations we have shown that presence of a penetrable matrix around the fracture with pulse flow rate, results in reduced pressure-drop compared to impenetrable matrixes. Therefore, we have suggested a friction coefficient (Eq. 6). Equation 6 shows that presence of a penetrable matrix around the fracture results in reduction of amount of friction coefficient compared to impenetrable matrixes.

CONCLUSION

In terms of numerical simulation, the single-phase and two-phase laminar flows were investigated considering presence of penetrable and impenetrable matrixes. The following results have been yielded from these simulations:

- Pressure drop calculated for the porous environment with pulse flow is 31% less than pressure-drop recorded for impenetrable matrix
- A considerable portion of pressure-drop takes place in areas with smallest diaphragms

- Presence of an impenetrable matrix surrounding the fracture results in reduction of friction coefficient in comparison with previous status of the impenetrable matrix
- A direct relationship exists between pressure-drop and flow rate. As the flow rate increases, pressure-drop increases as well

RECOMMENDATIONS

Regarding other issues related to this research, the following counts could be mentioned:

- Modeling of flow in turbulent flows and analysis of its effects on fracture matrix
- Three dimensional modeling of fracture flow in porous matrixes
- Modeling of a single-phase flow and investigation of heat conduction in saturated porous areas or investigation of inertia effects

REFERENCES

Barenblatt, G.I., I.P. Zeltov and I.N. Kochina, 1960. Basic concepts in the theory of seepage of homogeneous liquids in fissured rocks. J. Applied Math. Mech., 24: 1286-1303.

Berkowitz, B., 2002. Characterizing flow and transport in fractured geological media: A review. Adv. Water Resour., 25: 861-884.

Brush, D.J. and N.R. Thomson, 2003. Fluid flow in synthetic rough-walled fractures: Navier-Stokes, Stokes and local cubic law simulations. Water Resour. Res., 39: 1085-1099.

Chen, Z., S.L. Lyons and G. Qin, 2001. Derivation of the Forchheimer law via homogenization. Transp. Porous Media, 44: 325-335.

Court-Brown, C.M. and M.M. McQueen, 2002. The relationship between fractures and increasing age with reference to the proximal humerus. Curr. Orthopaedics, 16: 213-222.

Elsworth, D. and R.E. Goodman, 1986. Characterization of rock fissure hydraulic conductivity using idealized wall roughness profiles. Intl. J. Rock Mech. Mining Sci. Geomech. Abstr., 23: 233-243.

Koyama, T., I. Neretnieks and L. Jing, 2008. A numerical study on differences in using Navier-Stokes and Reynolds equations for modeling the fluid flow and particle transport in single rock fractures with shear. Intl. J. Rock Mech. Mining Sci., 45: 1082-1101.

Louis, C., 1969. A study of groundwater flow in jointed rock and its influence on the stability of rock masses, Imperial College. Rock Mech. Res. Rep., 10: 1-90.

Nazridoust, K., G. Ahmadi and D.H. Smith, 2006. A new friction factor correlation for laminar, single-phase flows through rock fractures. J. Hydrology, 329: 315-328.

Neuzil, C.E. and J.V. Tracy, 1981. Flow through fractures. Water Resour. Res., 17: 191-199.

Qian, J., H. Zhan, W. Zhao and F. Sun, 2005. Experimental study of turbulent unconfined groundwater flow in a single fracture. J. Hydrol., 314: 134-142.

Tsang, Y.W. and P.A. Witherspoon, 1981. Hydromechanical behavior of a deformable rock fracture subject to normal stress. J. Geophys. Res. Solid Earth, 86: 9287-9298.

Zimmerman, R.W. and G.S. Bodvarsson, 1996. Hydraulic conductivity of rock fractures. Transp. Porous Media, 23: 1-30.

Zimmerman, R.W., A. Al-Yaarubi, C.C. Pain and C.A. Grattoni, 2004. Non-linear regimes of fluid flow in rock fractures. Intl. J. Rock Mech. Mining Sci., 41: 163-169.